Quantification of Bound CO2 in various carbonated

Mickael Saillio, Véronique Baroghel Bouny, Matthieu Bertin, Julien Vincent, Jean-Baptiste D'espinose de Lacaillerie

QUANTIFICATION OF BOUND CO_2 IN VARIOUS CARBONATED CEMENTITIOUS MATRICES

M. Saillio[1], V. Baroghel-Bouny[2], M. Bertin[2], J. Vincent[1], J.B. de Lacaillerie[3]

ABSTRACT

For economic and ecological reasons, supplementary cementitious materials (SCM) are increasingly used in concrete. Although having a lot of advantages, these concretes have different cement matrices and do not have the same evolution as they are carbonated.

In this paper, comparison between various carbonated cement pastes with/without SCM (slag, fly ash and metakaolin), has been investigated. Samples are carbonated in accelerated conditions (1.5 % CO_2 , RH 65% and T=20°C) until constant mass but in order to be relatively close to the natural conditions and to simulate a carbonation process in the long term. The microstructure was characterized not only by usual techniques such as XRD and TGA-DTA, but also by ^{29}Si and ^{27}Al NMR spectroscopy. The use of a combination of techniques for microstructural characterization allows to quantify the proportion of each cementitious phase and to determine how much there are carbonated in comparison to reference cement pastes.

This quantification shows the evolution of the carbonated cementitious matrix as a function of the binder content. In addition, the results show that the quantity of bound CO_2 is not just dependent of portlandite amount. All phases with calcium participate to the fixation of CO_2. However, all these phases are not completely carbonated. Bound CO_2 is almost only $CaCO_3$. Four $CaCO_3$ polymorphs are detected : calcite, vaterite, aragonite and amorphous.

1. INTRODUCTION

Corrosion of reinforcement is one of the main causes of reinforced concrete degradation. This corrosion is due to carbonation or chloride ingress [1-5]. In CO_2-free environment, the hydrated Portland cement consists of hydrated phases in equilibrium with a pore solution whose pH is around 13.5. Under natural conditions of temperature and pressure, the atmospheric CO_2 is dissolved into the pore solution to form H_2CO_3 which, by dissociation, decreases the pH of the pore solution [1-8]. Portlandite ($Ca(OH)_2$) plays the role of buffer and maintains the pH of the pore solution at pH=12.5 by releasing adequately OH^- ions. During the carbonation process, the dissolution can affect not only $Ca(OH)_2$ but also C-S-H, AFm, AFt… [8-10].

The changes in cementitious materials induced by carbonation are particularly significant when the mixture contains supplementary cementitious materials (SCM) [8][11-17]. Binders which contain ground granulated blast furnace slag (GGBS) for example are used in marine

[1] Paris-Est University, MAST, CPDM, IFSTTAR, France; mickael.saillio@ifsttar.fr ; julien.vincent@ifsttar.fr
[2] Paris-Est University, MAST, CPDM, IFSTTAR, France; véronique.baroghel-bouny@ifsttar.fr ; matthieu.bertin@ifsttar.fr

environment since the chloride diffusion coefficient of GGBS-mixtures is significantly reduced. But these binders form less portlandite than OPC binders [8,12]. Consequently, for a same exposure environment and time, carbonation ingress in these materials is higher than in OPC binders [11] as also expected for binders with fly ash or metakaolin.

The aim of this research is to investigate the effect of carbonation on cementitious matrixes with SCM or not and, finally, to quantify how much each phase can bind CO_2.

2. EXPERIMENTAL

2.1 Materials studied

Various cement pastes were designed with the same clinker. The main constituents of the clinker are given in tables 1 and 2. The water to binder ratio (w/b) is equal to 0.50 for all the mixtures. The studied binders are CEM I (OPC with 97% clinker), CEM III/A (with 62% GGBS) denoted CEM III GGBS(62%), CEM III/C (with 82% GGBS) denoted CEM III GGBS(82%), CEM I + 20% FA denoted CEM I FA(20%), CEM I + 30% FA denoted CEM I FA(30%), CEM I + 40% FA denoted CEM I FA(40%), CEM I + 10% MK denoted CEM I MK(10%) and CEM I + 25% MK denoted CEM I MK(25%).

Table 1: Chemical compositions of the cements and SCM tested (in %)

	CaO	SiO_2	Fe_2O_3	Al_2O_3	TiO_2	MgO	Na_2O	K_2O	MnO	SO_3
CEM I	62.53	19.54	2.90	4.98	0.30	0.84	0.30	0.82	0.09	2.97
CEM III/A	49.77	29.86	1.28	8.10	0.46	4.61	0.40	0.56	0.16	2.29
CEM III/C	45.70	32.00	1.00	9.90	0.50	5.80	0.63	0.54	0.20	2.00
MK	2.00	66.29	4.29	21.30	1.12	0.25	0.84	0.49	0.00	0.08
FA	4.30	51.59	6.58	23.78	1.03	0.49	1.09	3.05	0.11	3.05

Table 2: Mineralogical composition of the CEM I from BOGUE calculation (in %)

	C_3S	C_2S	C_3A	C_4AF
CEM I	51.2	28.3	9.9	8.8

Sound samples (i.e. non-carbonated) will be denoted “Ref sample” in the paper.

2.2 Carbonation process

Accelerated carbonation tests are often used to carbonate samples in lab as an alternative technique to the natural carbonation process which is much longer [9,18]. Tests consist in, after drying, leaving samples in an environment enriched in CO_2 at an optimal relative humidity (40-65%) [18]. Different CO_2 concentrations can be applied in accelerated tests. According to [9], a too high concentration can change the microstructure more than a natural carbonation process would. A drying process increases carbonation ingress but a too high temperature alters cementitious phases such as ettringite. In this study, samples were carbonated in accelerated conditions.

The following carbonation protocols have been chosen: after water curing (365 days), slices of concretes or pastes are dried during 3 days at 60°C. Then the slices are crushed. A part of the crushed samples is preserved in CO_2-free environment (as “Reference samples”). The other part is carbonated in chamber (1.5% CO_2 and 65% RH), until constant mass (as “Totally Carbonated” sample).

2.3 Microstructural characterization

Combination of usual technics (XRD, TGA/DTA and NMR ^{29}Si and ^{27}Al) [18-35] are used in order to obtain the phase assemblage of the various cementitious matrices carbonated or not. These calculations notably take into account the dilution effect provided by contribution of CO_2 in order to calculate adequately each phase proportion. It was not possible to make the characterizations on all samples. We focus on 6 type of binder : CEM I, CEM I MK(10%), CEM I MK(25%), CEM I FA(30%), CEM III GGBS(62%) and CEM III GGBS(82%).

3. RESULTS AND DISCUSSION

$CaCO_3$ becomes the main phase in terms of weight for all TC samples (see figure 1). The mass proportion of $CaCO_3$ in the OPC sample is over 60%. It was expected that this sample contains more $CaCO_3$, since it had the highest amount of calcium (the CaO amount of the clinker was 62%). There is a linear relationship between the amount of $CaCO_3$ produced and the quantity of CaO in the anhydrous binders (see figure 2) depending of the SCM type. The difference between MK, FA and GGBS cement paste is probably because calcium is almost only in hydrated phase for the Ref samples with FA or MK in the opposite case of cement paste with GGBS, where calcium can be also in anhydrous phases (slag). Hydrated and anhydrous phases do not have the same reactivity to the carbonation (see figure 3). Nevertheless, carbonation of anhydrous phases (C_2S and C_3S) obviously can occur. In addition, accessibility can be an another explanation because there are differences between porous network as a function of SCM binders. According to the results, $CaCO_3$ forms at the expense of portlandite and other hydrated phases. Portlandite has disappeared in all TC sample (DTA results do not show any peak) nevertheless it continues to appear on the diffractograms (small peak) except for CEM III GGBS(62%) and CEM III GGBS(82%) (see figure 4). Therefore, in the other samples, the carbonation process has not completely consumed portlandite. In this case, the formation of calcium carbonate on the surface of portlandite crystals probably limits calcium dissolution from portlandite as reported [18,35]. In addition, figure 1 show decreasing of all phases (excepted $CaCO_3$). Nevertheless, there is a mass contribution by the CO_2 arrival that causes a dilution phenomenon in carbonated materials for all the phase containing no CO_2. Figure 3 takes into account this dilution effect by reporting the amounts of each phase to the initial amount of clinker. The results confirm indeed that almost all phases decrease by degradation under carbonation and not only by dilution effect.

TGA allows to have the total amount of $CaCO_3$ produced (orange lines in figure 10). This amount can also be calculated by accounting the lost calcium for each of the sample phases that have been degraded between the Ref and TC sample (taking account the dilution effect) (see figure 5). When comparing the both results on the same figure, the overall amount obtained directly by TGA is higher for some samples than that calculated for each degraded phase. This means that the decalcification of certain phases such as aluminate phases is minimized and also some phases which contain calcium (TAH, C_3A, C_4AF …) are not taking into account. In addition, some of these phases may remain their structure even they are

decalcified and therefore they still appear in NMR spectroscopy in the form of AFm and AFt phases.

In XRD pattern of carbonated samples (see figure 4), vaterite (peak at 3.28Å), calcite (peak at 3.08Å) and aragonite (peak at 3.39Å) are recorded as the main crystalline phases as already observed by previous studies [4,6,9]. The polymorphism of $CaCO_3$ crystal depends on the cementitious phase from which it was formed, the pH of the pore solution and on the temperature [36,37]. Portlandite generally induces the formation of calcite while the other phases (C-S-H and aluminates phases) form vaterite and aragonite which evolve to calcite with time [37]. This is in agreement with the present study. In fact, the Rietveld analysis applied to the TC CEM I paste shows that there are 38% of crystalized $CaCO_3$ in the form of vaterite, 41% as aragonite and 21% as calcite, while the proportions for the CEM III GGBS(82%) sample are 94% as vaterite, 1% as aragonite and 5% as calcite. According to figure 5, calcium present in $CaCO_3$ comes mainly from C-S-H for CEM III GGBS (only 2% of portlandite in Ref CEM III GGBS(82%) vs 18% in Ref CEM I), while the source of calcium is shared between C-S-H and portlandite in the case of the CEM I sample. This confirms that vaterite is formed from the C-S-H and that its presence is an indicator of the degradation (decalcification) of the C-S-H. However, aragonite amount is high in almost TC sample (except CEM III with GGBS) and it can not be explain only by the origin of the phases. Carbonation conditions (RH, T, level of CO_2, the duration,…) of cement paste can also influence the phase assemblage [36,37]. Finally, XRD and specially TGA results seem to indicate there is amount of amorphous $CaCO_3$ (in addition to crystalized forms) which can not be quantified, consequently it is not possible to determinate precisely each phase of $CaCO_3$ and the values of Rietveld analysis given below are at best semi-quantitative.

Other informations on cementitious matrices can be obtain with these results (see figure 6, 12). As said previously, the significant presence of vaterite and aragonite shows that there is degradation of the C-S-H and probably of the aluminate phases, since the amounts of ettringite and AFm decrease according to ^{27}Al NMR results (see figure 6). Aluminium from AFm and AFt phases moves to tetrahedral configuration phases. For example, the CEM III GGBS(82%) TC sample has 80% of its aluminum in tetrahedral configuration instead of 42% in the case of Ref sample. It seems that aluminum from decalcified AFm and AFt phases is incorporated into the C-S-H probably decalcified as silica gel.

The average lengths of the C-S-H chains increase for all TC samples (see figure 7). Furthermore, the degradation products C-S-H (Q^3+Q^4) also increase at the expense of the amount of C-S-H (Q^1+Q^2) (see example in figure 7). The C-S-H chains polymerize to form a substantial silica gel. The deconvolution of the ^{29}Si NMR spectra of carbonated samples also shows the possible presence of Q^4(1Al) or even Q^3(1Al), in addition to the Q^4 and Q^3 species. Q^4(1Al) represents silicon surrounded by four neighbours where one is aluminum, confirming thereby the ^{27}Al NMR results. The hydration rate of TC samples (obtained by ^{29}Si NMR) increases but no C-S-H is formed. Despite a weak accessibility, C_3S and C_2S phases seem to be partially decalcified. As expected, calcium amount of the C-S-H decreases in all TC samples (see figure 3) confirming thereby the massive decalcification of the C-S-H (over 60% of calcium moved).

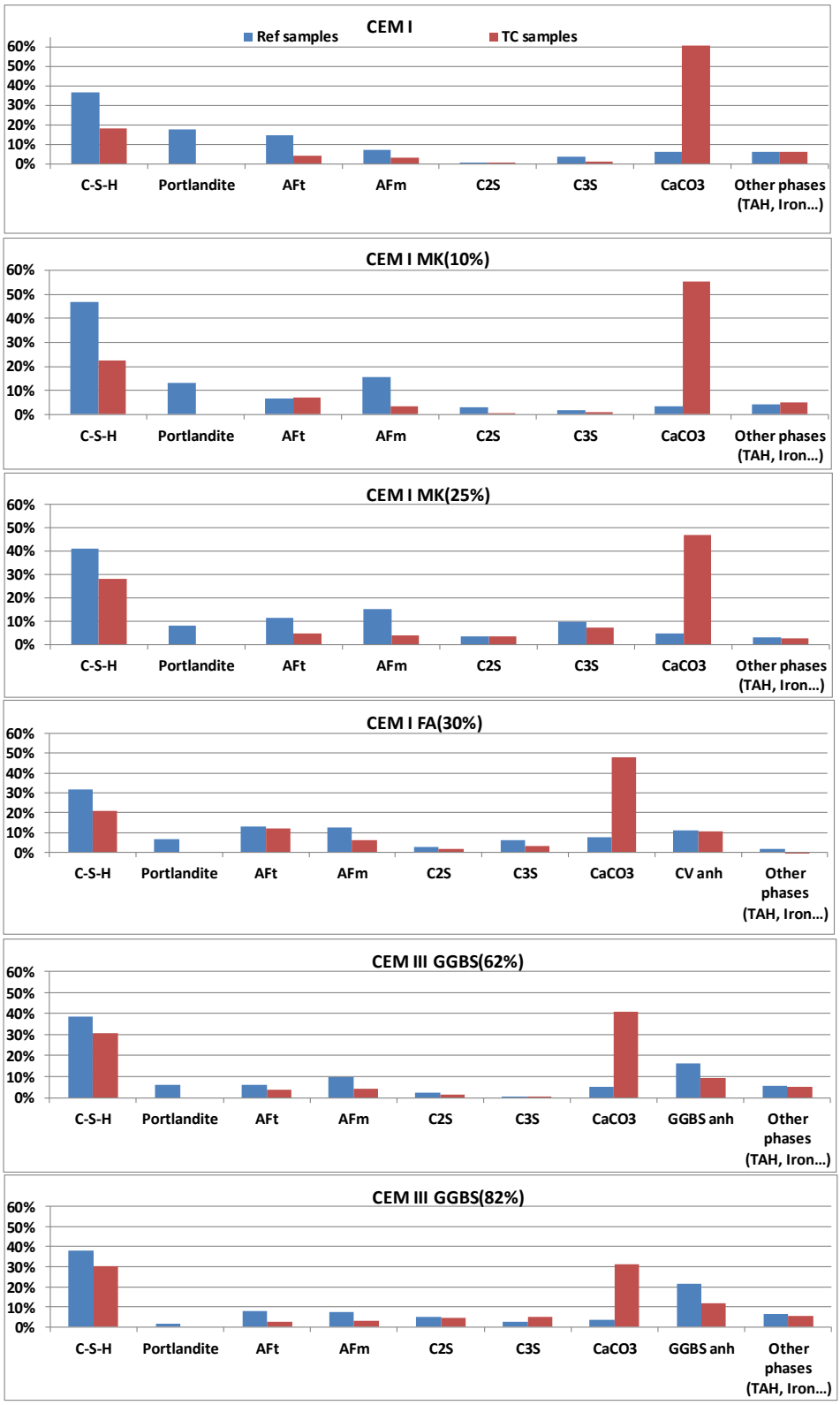

Figure 1: Comparisons of mass proportion between Ref and TC samples. TC samples were carbonated until constant mass in chamber at 1.5% CO2 and 65% RH, after 365-day water curing. Here C-S-H= C-S-H+silica gel.

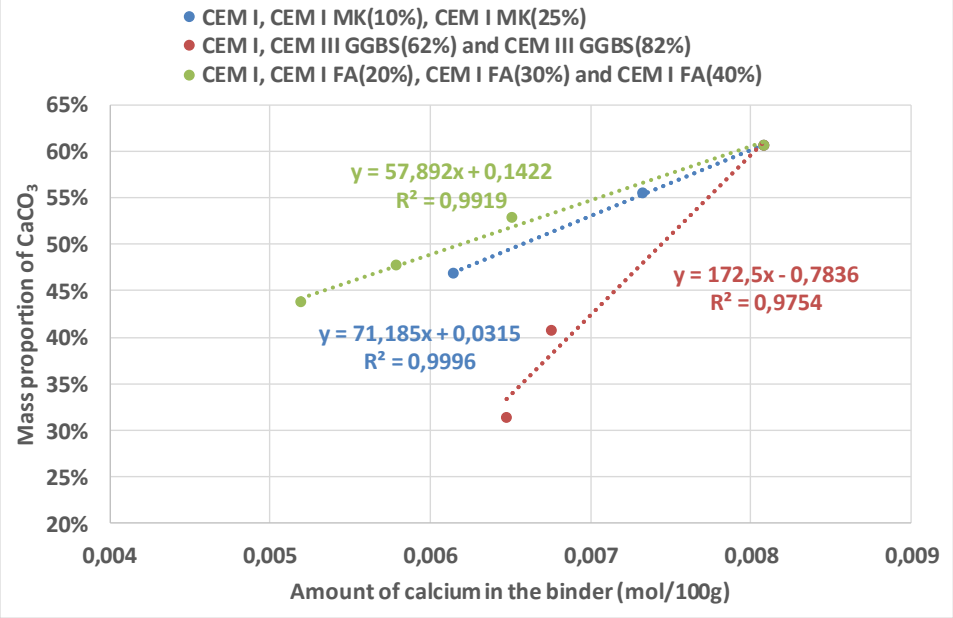

Figure 2: Comparison between the proportion of calcium in the binder and the mass proportion of $CaCO_3$ of the samples. TC samples were carbonated until constant mass in chamber at 1.5% CO_2 and 65% RH, after 365-day water curing.

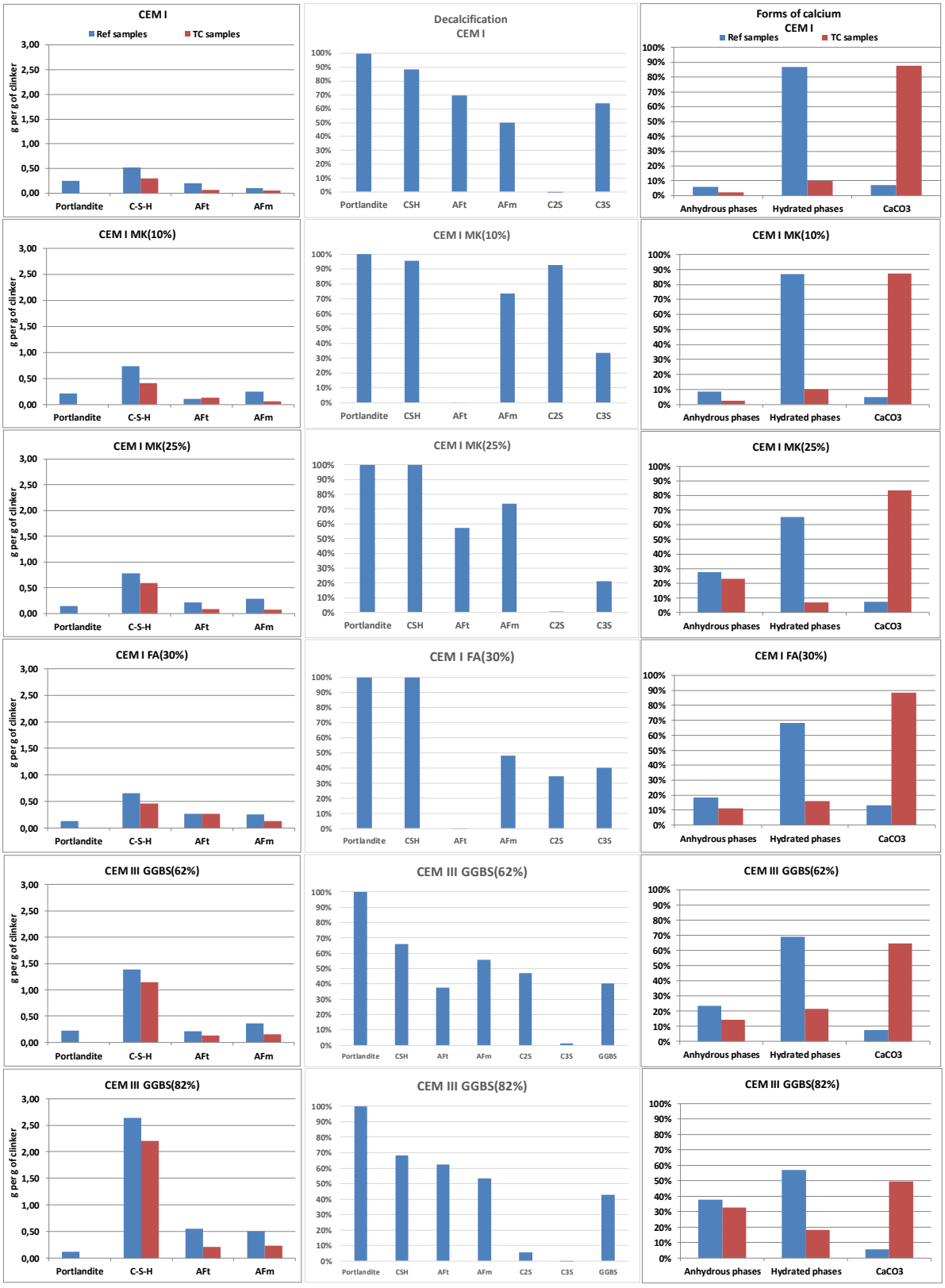

Figure 3: Mass proportion reported to clinker (in left), decalcification of each phase (in middle) and forms of calcium in cement pastes.

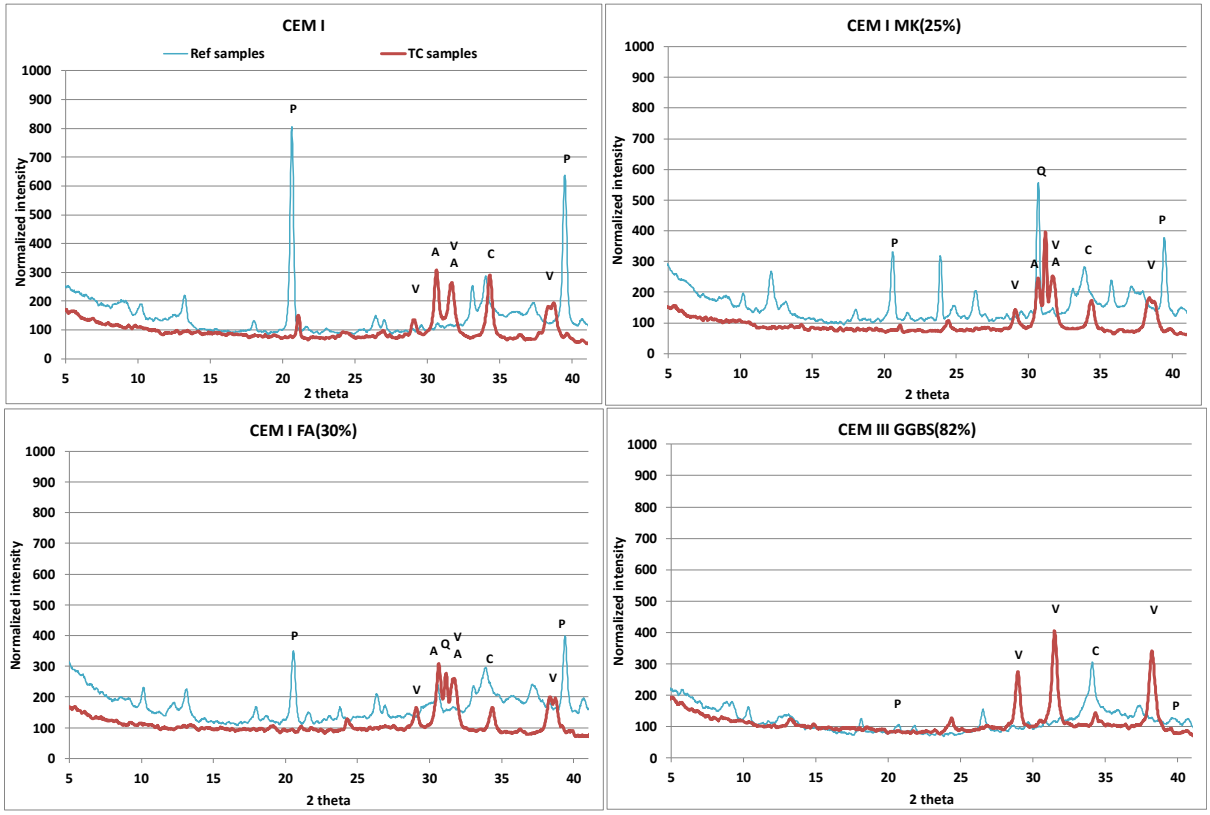

Figure 4: Partial XRD patterns of cement pastes for Ref and TC samples. TC samples were carbonated until constant mass in chamber at 1.5% CO2 and 65% RH after 365-day water curing. Portlandite (P), calcite (C), vaterite (V), aragonite (A), quartz (Q).

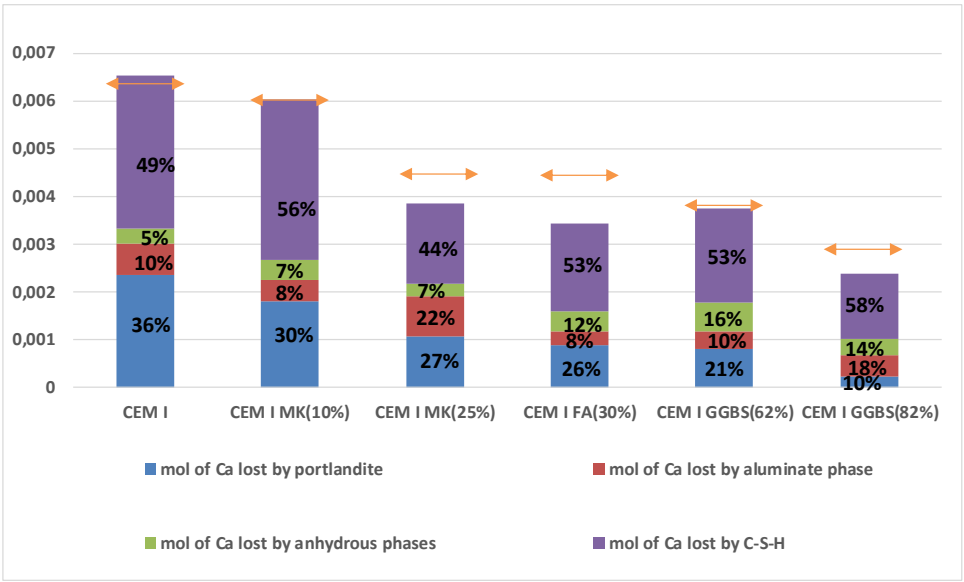

Figure 5: Amount of calcium in $CaCO_3$ produced as a function of each phases for TC samples compared to the total amount of $CaCO_3$ produced during carbonation.

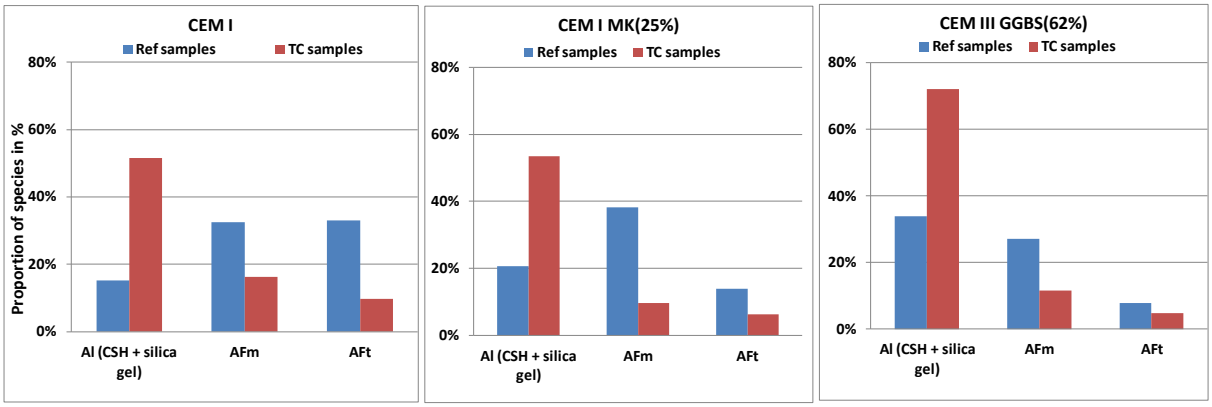

Figure 6: Proportion of Al species in cement pastes before and after total carbonation (carbonation until constant mass in chamber at 1.5% CO2 and 65% RH, after 365-day water curing), obtained by 27Al NMR.

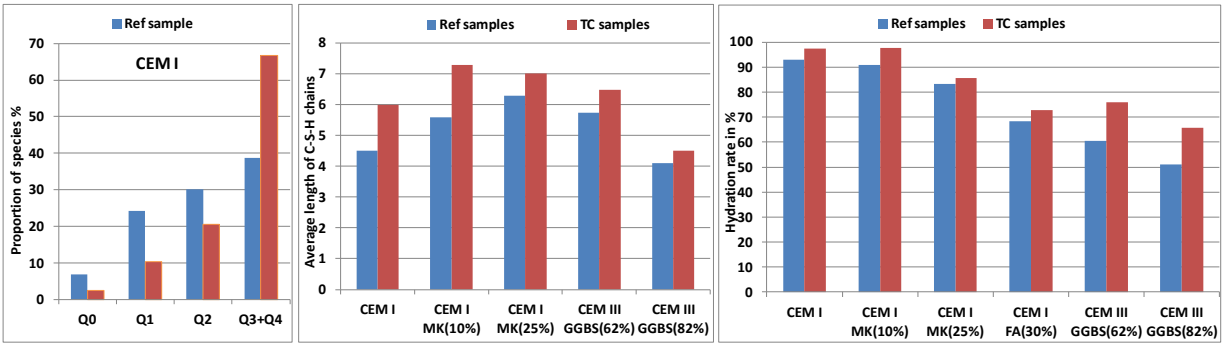

Figure 7: Hydration rate and average length of C-S-H chains obtained 29Si by NMR for reference (Ref) samples and totally carbonated (TC) ones (carbonation until constant mass in chamber at 1.5% CO2 and 65% RH) after 365-day water curing.

4. CONCLUSION

In this paper, quantification of each mineral phase has been obtained by combination of various techniques (XRD, DTG/TGA and ^{29}Si and ^{27}Al NMR MAS spectroscopy). The effect of total carbonation on the cement pastes was investigated for all cementious phases. Consequently, bound CO_2 amount can be quantified.

Total carbonation modifies all the hydrated phases. In totally carbonated CEM III with GGBS, there is no more portlandite (or just few traces depending on cement type). There is a linear relationship between the amount of $CaCO_3$ produced and the percentage of CaO in the anhydrous binders but also depending of the SCM type. The crystalline type of $CaCO_3$ depend also of the initial binder. Nevertheless, the decalcification is not complete for the other phases than portlandite, probably as a result of a weak accessibility (in the case of anhydrous phases)

or maybe a lower reactivity to carbonation. C-S-H and aluminate phases tend to become an aluminosilicate gel in all carbonated materials.

ACKNOWLEDGEMENTS

The authors are grateful to G.Platret and B.Duchesne from IFSTTAR (France) for XRD and TGA/DTG investigations, to J.B.D'Espinose de Lacaillerie from ESPCI (France) for NMR experiments and to P.Gegout and F.Barberon from Bouygues-TP for materials and for the founding of this study.

REFERENCES

[1] Cowie, J., Glasser, FP., The reaction between cement and natural waters containing dissolved carbon dioxide, Advances in Cement Research 4 (1992) 119-134
[2] Pollet, V., Dooms, B., Mosselmans G., Prevention of corrosion of the reinforcing bars by carbonation N°15, *in French*, (2007)..
[3] Nguyen, TQ., Petkovic, J., Dangla, P., Baroghel-Bouny, V., Modelling of coupled ion and moisture transport in porous building materials, Construction and Building Materials 22 (2008) 2185-2195.
[4] Balonis, M., Lothenbach, B., Le Saout, G., Glasser FP., Impact of chloride on the mineralogy of hydrated Portland cement systems, Cement Concrete Research 40 (2010) 1009-1022.
[5] Rasheeduzzafar, S., Ehtesham-Hussain, E., Effect of cement composition on chloride binding and corrosion of reinforcing steel in concrete, Cement and Concrete Research 21 (1990) 777-794.
[6] Sauman, Z., Lach, V., Long term carbonation of the $3CaO.Al_2O_3.6H_2O$ and $3CaO.Al_2O_3.SiO_2.4H_2O$, Cement and Concrete Research 4 (1972) 453-446.
[7] Ngala, VT., Page, CL., Effects of carbonation on pore structure and diffusionnal properties of hydrated cement pastes, Cement and concrete research 27 (1997) 995-1007.
[8] Borges, PHR., Costa, JO., Milestone NB., Lynsdale CJ., Carbonation of CH and C-S-H in composite cement pastes containing high amounts of BFS, Cement and Concrete Research 40 (2010) 284-292.
[9] Castellote, M., Fernandez, L., Andrade, C., Alonso, C., Chemical changes and phase analysis of OPC pastes carbonated at different CO_2 concentrations, Cement and Concrete Research 43 (2009) 515-525.
[10] Goni, S., Guerrero A., Accelerated carbonation of Friedel's salt in calcium aluminate cement paste, Cement and Concrete Research 33 (2003) 21-26.
[11] Borges, PHR., Costa, JO., Milestone NB., Lynsdale CJ., Carbonation of CH and C-S-H in composite cement pastes containing high amounts of BFS, Cement and Concrete Research 40 (2010) 284-292.
[12] Leeman, A., Nygaard, P., Kaufman, J., Loser, R., Relation between carbonation resistance, mix design and exposure of mortar and concrete, Cement and Concrete Composites 62 (2015) 33-43.
[13] Taylor, R., Richardson, I., Brydson, R., Composition and microstructure of 20-year-old ordinary Portland cement-ground granulated blast-furnace slag blends containing 0 to 100% slag, Cement and Concrete Research 40 (2010) 971-983.

[14] Girao, A., Richardson, I., Taylor, R., Brydson R, Composition, morphology and nanostructure of C-S-H in 70% white Portland cement-30% fly ash blends hydrated at 55 °C, Cement and Concrete Research 40 (2010) 1350-1359.
[15] Love, C., Richardson, I., Brough A., Composition and structure of CSH in white portland cement -20% metakaolin pastes hydrated at 25°C, Cement and Concrete Research 37 (2007) 109-117.
[16] Scrivener, K., Nonat, A., Hydration of cementitious materials, present and future, Cement and Concrete research 41 (2011) 651-665.
[17] Wang, XY., Lee HS., Modeling the hydration of concrete incorporating fly ash or slag, Cement and Concrete Research 40 (2010) 984-996.
[18] Villain, G., Thiery, M., Platret, G., Measurement of carbonation profiles in concrete: Thermogravimetry, chemical analysis and gammadensimetry, Cement and Concrete Research 37 (2007) 1182-1192.
[19] Engelhardt, G., Michel D., High resolution ^{29}Si NMR of silicates and Zeolites. Wiley, New York; (1987).
[20] Jones, MR., Macphee, DE., Chudek, JA., Hunter, G., Lannegrand, R., Talero, R., Scrimgeour, SN., ^{27}Al MAS NMR of AFm and AFt phases and the formation of Friedel's salt, Cement and Concrete Research 33 (2003) 177-182.
[21] Sun, GK., Young, JF., Kirkpatrick RJ., The role of Al in C-S-H: NMR, XRD, and compositional results for precipitated samples, Cement and Concrete Research 36 (2006) 18-29.
[22] Andersen, MD., Jakobsen HJ., Skibsted J., A new aluminium-hydrate species in hydrated Portland cements characterized by 27Al and 29Si MAS NMR spectroscopy, Cement and Concrete Research 36 (2006) 3-17
[23] Skibsted, J., Henderson E., Jakobsen HJ., Characterization of calcium aluminate phases in cements by ^{27}Al MAS NMR spectroscopy, Inorganic Chemistry 32 (1993) 1013-1027.
[24] Beaudoin, JJ., Dramé, H., Laila, R., Alizadeh, R., Formation and properties of C-S-H-PEG nano-structures, Materials and Structures 42 (2009)1003-1014.
[25] Thomas, JJ., Allen, AJ., Jennings H., Density and water content of nanoscale solid C–S–H formed in alkali-activated slag (AAS) paste and implications for chemical shrinkage, Cement and Concrete Research 42 (2012) 377-383
[26] Richardson, IG., The nature of C-S-H in hardened cements, Cement and Concrete Research 29 (1999) 1131-1147.
[27] Saillio, M., Baroghel-Bouny, V., Bertin, M., Pradelle, S., Vincent, J., Phase assemblage of cement pastes with SCM at different ages, *under review*, Construction and Building Materials (2019).
[28] Peter, M., Muntean, A., Meier, S., Bohm, M., Competition of several carbonation reactions in concrete: a parametric study, Cement and Concrete Research (2008) 1385-1393.
[29] Parott, LJ., Review of carbonatation of concrete, British Cement Association, Londres, (1987).
[30] Taylor, W., Cement chemistry, Londres: academic press, (1997).
[31] Dilnesa, B., Lothenbach, B., Le Saout, G., Renaudin, G., Mesbah, A., Filinchuck Y., Iron in carbonate containing AFm phases, Cement and Concrete Research 41 (2011) 311-323.
[32] Utton, C., Gallucci, E., Hill, J., Milestone, N., Interaction between BaCO3 and OPC/BFS composite cements at 20°C and 60°C, Cement and Concrete research 41 (2011) 236-243.

[33] Saillio, M., Baroghel-Bouny, V., Chloride binding in sound and carbonated cementitious materials with various types of binder, Construction and Building Materials 68 (2014) 82-91.
[34] Saillio, M., Baroghel-Bouny, V., Pradelle, S., Various durability aspects of calcined Kaolin-Blended Portland cement pastes and concretes, Proceedings of Calcined clays for sustainable concrete, Lausanne, RILEM Bookseries 10 (2015) 491-499.
[35] Rafai, N., Hornain, H., Villain, G., Baroghel-Bouny, V., Platret, G., Chaussadent, T., Comparison and validity of the carbonation methods *in french*, RFGC 6 (2002) 251-274.
[36] Tai, C., Chen, S., Nucleation, aglomeration and cristal morphology of calcium carbonate, AIChE Journal 41 (1995) 68-77.
[37] Drouet, E., Impact of temperature on carbonation process of cementitious materials, *in French*. Ph.D Thesis, Cachan (2010).
[38] Sevelsted, T., Skibsted J., Carbonation of C-S-H and C-A-S-H samples studied by ^{13}C, ^{27}Al and ^{29}Si MAS NMR spectroscopy, Cement and Concrete Research 71 (2015) 56-65.